

Litchi chinensis Peel: A Novel Source for Synthesis of Gold and Silver Nanocatalysts



Shriya Shende¹, Komal A Joshi², Anuja S Kulkarni³, Vaishali S Shinde³, Vijay Singh Parihar⁴, Rohini Kitture⁵, Kaushik Banerjee⁶, Narayan Kamble⁶, Jayesh Bellare⁷ and Sougata Ghosh^{1*}

¹Department of Microbiology, Modern College of Arts, Science and Commerce, Ganeshkhind, Pune-411016, India

²Institute of Bioinformatics and Biotechnology, Savitribai Phule Pune University, Pune-411007, India

³Department of Chemistry, Savitribai Phule Pune University Pune University, Pune-411007, India

⁴Department of Biomedical Sciences and Engineering, BioMediTech, Tampere University of Technology, Korkeakoulunkatu 10, 33720, Tampere, Finland

⁵Department of Applied Physics, Defense Institute of Advanced Technology, Girinagar, Pune-411025, India

⁶National Referral Laboratory, ICAR-National Research Centre for Grapes, Manjri Farm, Pune-412307, India

⁷Department of Chemical Engineering, Indian Institute of Technology, Bombay, Powai, Mumbai-400076, India

Submission: August 19, 2017; **Published:** September 21, 2017

***Corresponding author:** Dr. Sougata Ghosh, Department of Microbiology, Modern College of Arts, Science and Commerce, Ganeshkhind, Pune 411016, India, Email: ghoshsibb@gmail.com

Abstract

Nanosized metal particles are very significant due to their chemical, physical and biological applications which emphasizes the need to design more efficient, economical, rapid, eco-friendly processes. Herein we report the use of medicinal plant, *Litchi chinensis* for synthesis of silver (AgNPs) and gold nanoparticles (AuNPs). Synthesis of AgNPs and AuNPs was completed within 5h which showed prominent peaks at 430nm and 540nm respectively. Higher temperature of 50 °C and 5mM concentration of respective salt solution facilitated a faster rate of synthesis. AgNPs synthesized by LCPE were found to be mostly spherical ranging from 10 to 20nm while diversity in shapes of AuNPs included nano-hexagons, pentagons and trapezoids in a range of 30 to 60nm. Particles were further characterized and confirmed using EDS, DLS and XRD. FTIR analysis revealed broad peak at ~ 3350cm⁻¹ indicating the hydroxyl (-OH) group of phenols/alcohol in LCPE. Phytochemical analysis confirmed the presence of polyphenols, starch, reducing sugars, ascorbic acid and citric acid that might play a vital role in reduction and stabilization process. GCMS/MS fingerprinting exhibited the presence of diverse phytochemicals in LCPE like erucic acid, geranyl isovalerate, 2-hexadecanol, α -acorenol and tetradecane. Both AgNPs and AuNPs showed significant catalytic potential in conversion of 4-nitrophenol to 4-aminophenol by NaBH₄ following a pseudo-first order rate kinetics with the apparent rate constant (k) 2.369 x 10⁻⁴ min⁻¹ and 1.356 x 10⁻⁴ min⁻¹, respectively.

Keywords: *Litchi chinensis*; Gold nanoparticles; Silver nanoparticles; Gas chromatography Mass spectroscopy fingerprinting; Chemical catalysis

Introduction

Development of green synthetic process for nanoparticles has gained attention recently due to the increase in applications of nanoparticles, particularly nanomedicine [1-4]. Available chemical processes involve chemicals which are toxic and hazardous to the environment. Among various nanoparticles gold and silver nanoparticles have got wide attention owing to their immense utility. Gold nanoparticles (AuNPs) are widely used in electronics, sensors, catalysis, drug delivery, diagnostics, medicine due to their unique optical, physical, chemical, and

magnetic properties [5-8]. Similarly, silver nanoparticles (AgNPs) are studied most extensively as antimicrobial agent and are reported as most potent antibacterial and antiviral nanomaterial [9]. Hereby, novel biological routes for synthesis of metal nanoparticles using bacteria, fungi and plants needs to be explored to assure its biocompatibility and reduced toxicity. Medicinal plants are considered to be rich source of diverse groups of phytochemicals which not only help in the reduction procedure of the metal ions but also help in stabilization

of the bioreduced nanoparticles [10-15]. Medicinal plants like *Dioscorea bulbifera*, *Gnidia glauca*, *Plumbago zeylanica*, *Gloriosa superba*, *Barleria prionitis* and *Dioscorea oppositifolia* are reported to synthesize metal nanoparticles with various biomedical applications [16-21].

Similarly, *Litchi chinensis* is a medicinal plant which is reported to possess various medicinal properties like antioxidant, antidiabetic, anti-inflammatory, analgesic and antipyretic activities [22,23]. However, till date there are no reports on the catalytic potential of the AuNPs and AgNPs synthesized by *L. chinensis* peel extract (LCPE). In view of this background, herein we report for the first time an optimized process for synthesis of AgNPs and AuNPs employing LCPE. Further, the bioreduced nanoparticles were characterized using UV-visible spectroscopy, high resolution transmission electron microscopy (HRTEM), energy dispersive spectroscopy (EDS), dynamic light scattering (DLS), X-ray diffraction spectroscopy (XRD). We also report the phytochemical constituents present in LCPE that might be responsible for both reduction and stabilization of AgNPs and AuNPs. Further, the catalytic potential of the biogenic nanoparticles were evaluated by motoring the chemical reduction of 4 nitrophenol (4-NP) to 4 aminophenol (4-AP).

Materials and Methods

Plant material and preparation of extract

L. chinensis peel were collected and dried in shade at room temperature for 2-3 days. The dried peels were pounded into fine powder in an electric blender. LCPE was prepared by boiling 5g of peel powder in 100mL distilled water for 5min. After centrifugation at 3000 rpm for 10min the supernatant was filtered through Whatman No.1 filter paper. The filtrate was collected and stored at 4 °C for further use [19].

Synthesis and characterization of silver and gold nanoparticles

5mL of LCPE was added in 95mL of 1mM AgNO₃ to initiate the synthesis of AgNPs. Thorough mixing was confirmed by shaking the reaction mixture at 40 °C for 5 h in a shaker incubator. Reduction of Ag⁺ ions to AgNPs was indicated by visible colour change followed by UV-visible spectrometry at regular intervals. Similarly, 5mL of LCPE was added into 95mL of 1mM HAuCl₄ solution for synthesis of AuNPs. Conditions were optimized to achieve maximum synthesis of both AgNPs and AuNPs. Temperature optimization was carried out in a water bath at 4 °C-50 °C with reflux while concentration optimization was done by varying the respective salt concentration from 0.3 to 5mM. The bioreduced nanoparticles were characterized employing high resolution transmission electron microscopy (HRTEM), energy dispersive spectroscopy (EDS), X-ray diffraction (XRD)

and fourier transform infrared spectroscopy (FTIR) as per our earlier reports [20].

Phytochemical analysis

Total phenolic, starch, reducing sugar, ascorbic acid and citric acid in LCPE were estimated using biochemical assays reported earlier. Similarly, identification of the principle phytochemicals present in LCPE was carried out using GC-MS/MS fingerprinting [21].

Catalytic activity

The catalytic reduction of 4 nitrophenol (4-NP) to 4 aminophenol (4-AP) was carried out using UV-vis spectroscopy at 25 °C in a quartz cuvette with an optical path length of 1cm and volume 4.5ml. Freshly prepared 0.1mL of NaBH₄ (0.1M) solution was added to aqueous solution of 4-NP (2mL, 0.1 mM). Thereafter, 50µL of suspension containing metal nanoparticles (10 mM) were added to the solution and the absorbance was measured. The change in absorbance was measured in situ to obtain the successive information about the reaction. Completion of reaction was indicated by the change in color from yellow to colourless [18-20].

Results

UV-visible spectroscopy

Synthesis of nanoparticles was indicated by the visible colour change in the reaction mixture on addition of the LCPE in the respective salt solution. AgNO₃ solution first turned into pale yellow which gradually turned into intense brown on incubation till 5h. Further UV-visible spectrometry showed a gradual peak build up at 430nm from 0 to 5h beyond which no further increase in the intensity was observed which indicated that synthesis of AgNPs completes at 5 h (Figure 1A). Similarly in case of AuNPs, initially the reaction mixture turned pale red followed to which it gradually changed to intense ruby red in colour. The synthesis was very fast and the colour started developing instantly on addition of LCPE to HAuCl₄ solution. The reaction almost completed by 2h as maximum increase in the peak intensity at 540 nm was observed from 0 to 2 h followed to which very less increase at 3h, 4h and 5h (Figure 1B)

Temperature optimization studies revealed that till 30 min no difference was observed in the rate of synthesis of the AgNPs at different temperature, while after that a sharp increase in the rate of synthesis was evident at 50 °C (Figure 2A). Similarly, even for synthesis of AuNPs, higher temperature of 50 °C was found to be optimum for synthesis (Figure 2B). In case of concentration optimization among various concentrations of AgNO₃, 5mM was found to be optimum followed by 3mM for synthesis of AgNPs (Figure 3A). Likewise, for AuNPs as well, 5mM of HAuCl₄ was found to be optimum for synthesis using LCPE (Figure 3B).

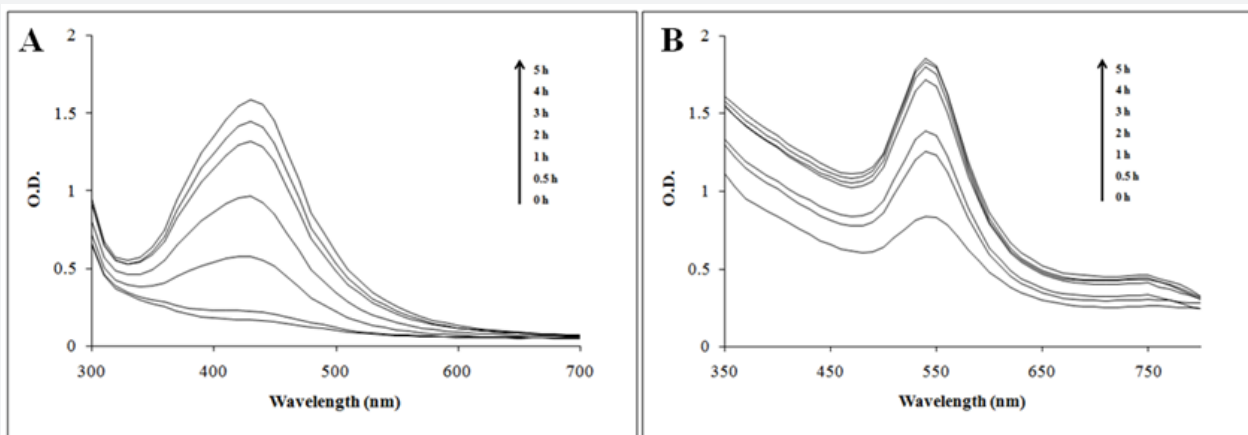


Figure 1: UV-vis spectra recorded as a function of reaction time for nanoparticle formation using LCPE at 40°C with (A) 1mM AgNO₃ solution and (B) HAuCl₄ solution.

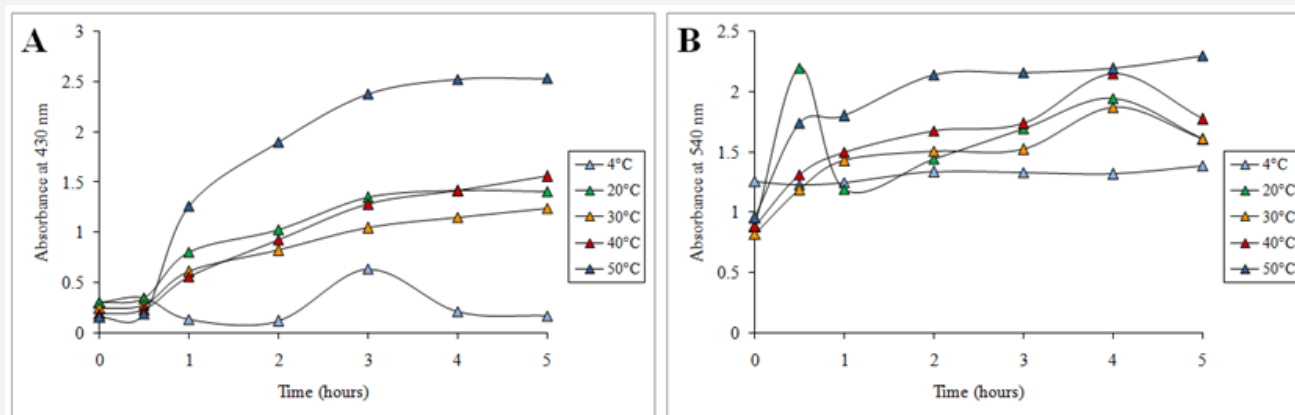


Figure 2: Time course of nanoparticle synthesis using LCPE at different reaction temperatures with (A) 1 mM AgNO₃ and (B) 1 mM HAuCl₄.

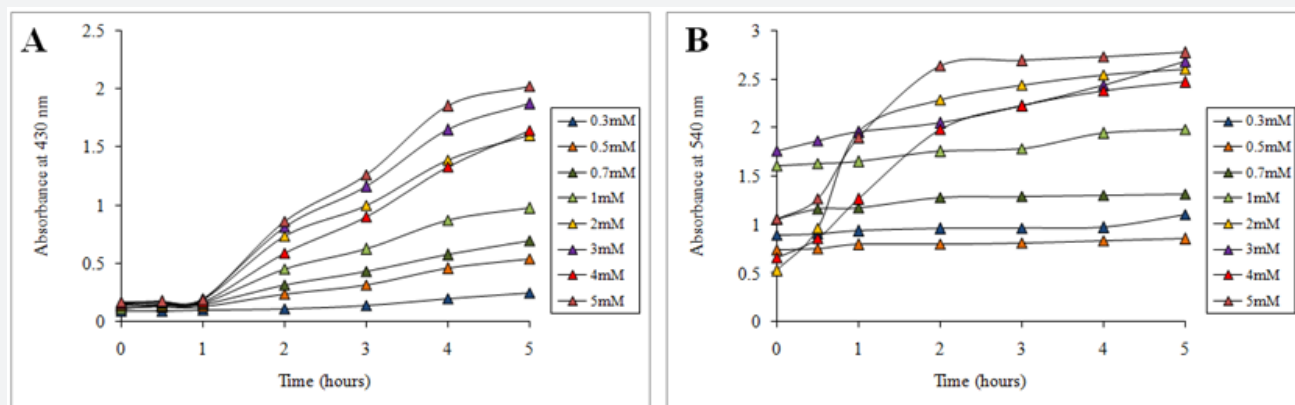


Figure 3: Time course of nanoparticle synthesis using LCPE at 40 °C with (A) different concentrations of AgNO₃ and (B) HAuCl₄.

HRTEM, EDS, DLS analysis

HRTEM analysis showed that majority of the AgNPs synthesized by LCPE are monodispersed and spherical in shape. The bioreduced AgNPs ranged between 10 to 20nm. The particles were found to be fairly stable with no larger aggregates. AgNPs were well dispersed either as single particles or were found in a group of 2 to 4 particles (Figure 4A & Figure 4B). Anisotropic

AuNPs with exotic shapes were visible in HRTEM. Nanospheres, hexagons, trapezoids and pentagonal nanoparticles were observed (Figure 5A and Figure 5B). The particles were discrete, separate and well dispersed with no visible agglomeration. This indicates the stability and polydispersity of the AuNPs bioreduced by LCPE. EDS spectra confirmed the presence of elemental silver and gold in the AgNPs and AuNPs, respectively

(Figure 5A & 5B). Particle size distribution recorded using dynamic light scattering for AgNPs and AuNPs synthesized using LCPE was found to be well in agreement with the HRTEM results (Figure 6A & 6B). Figure 7A & Figure 7B represent the XRD pattern of AgNPs and AuNPs, respectively. The obtained data was compared with the standard powder diffraction data released by Joint Committee for Powder Diffraction Standards (JCPDS). The peak positions for the standard lattice planes (111), (200), (220) and (311) of Ag and Au nanoparticles were matching with their respective standard values as mentioned in the JCPDS data card no. 04-0783 and 04-0784, respectively, confirming the phase formation of the nanoparticles. The cubic structure of the AgNPs and AuNPs indicate the standard lattice constant to be 4.086 Å and 4.078 Å, respectively. In an attempt to understand the chemistry behind the reduction of metal salt with the help of LCPE, the FTIR spectra, before and after reduction of the salts Ag^+ and Au^{3+} , respectively, were recorded (Figure 8). The shift/disappearance of characteristic peaks of the original LCPE, after the reduction of metal salts into the nanoparticles could indicate the possible group active in reduction. The broad peak at $\sim 3350\text{ cm}^{-1}$ indicates the hydroxyl (-OH) group of phenols/alcohol. The peaks at $\sim 1610\text{ cm}^{-1}$ did not show any prominent shift which is attributed to the C=C group. The peak of the LCPE at 2923 cm^{-1} (C-H stretch) is seen to be diminished while new peaks appeared at 1739 cm^{-1} .

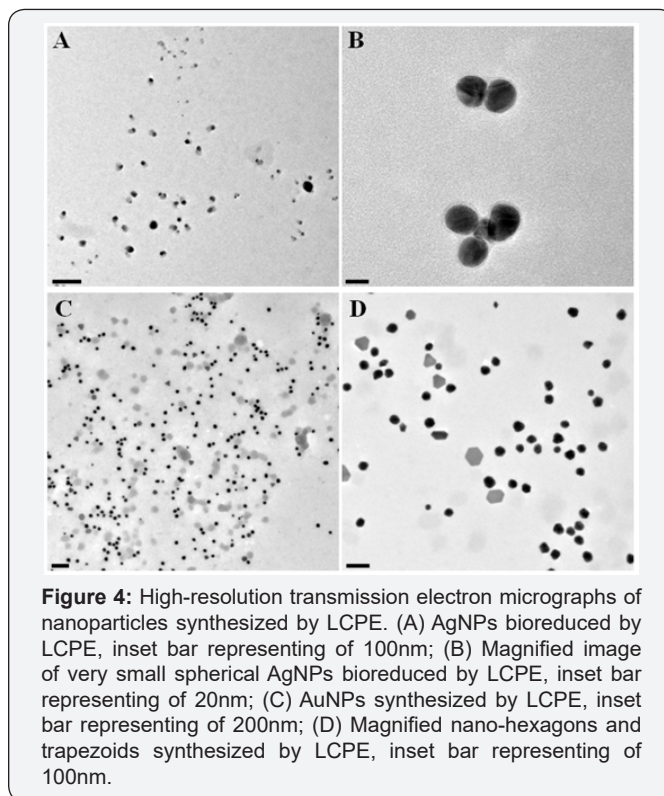


Figure 4: High-resolution transmission electron micrographs of nanoparticles synthesized by LCPE. (A) AgNPs bio-reduced by LCPE, inset bar representing of 100nm; (B) Magnified image of very small spherical AgNPs bio-reduced by LCPE, inset bar representing of 20nm; (C) AuNPs synthesized by LCPE, inset bar representing of 200nm; (D) Magnified nano-hexagons and trapezoids synthesized by LCPE, inset bar representing of 100nm.

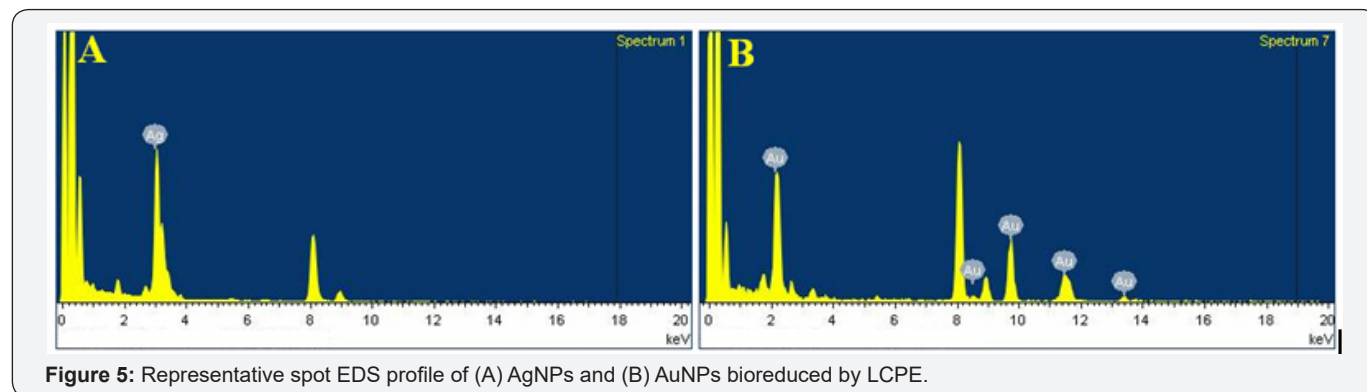


Figure 5: Representative spot EDS profile of (A) AgNPs and (B) AuNPs bio-reduced by LCPE.

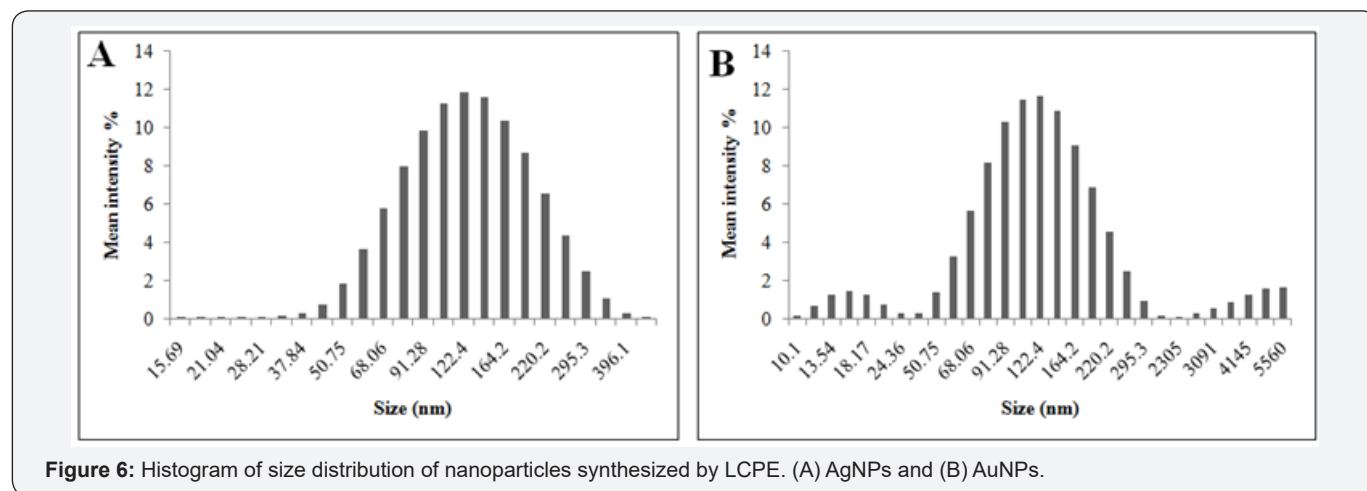


Figure 6: Histogram of size distribution of nanoparticles synthesized by LCPE. (A) AgNPs and (B) AuNPs.

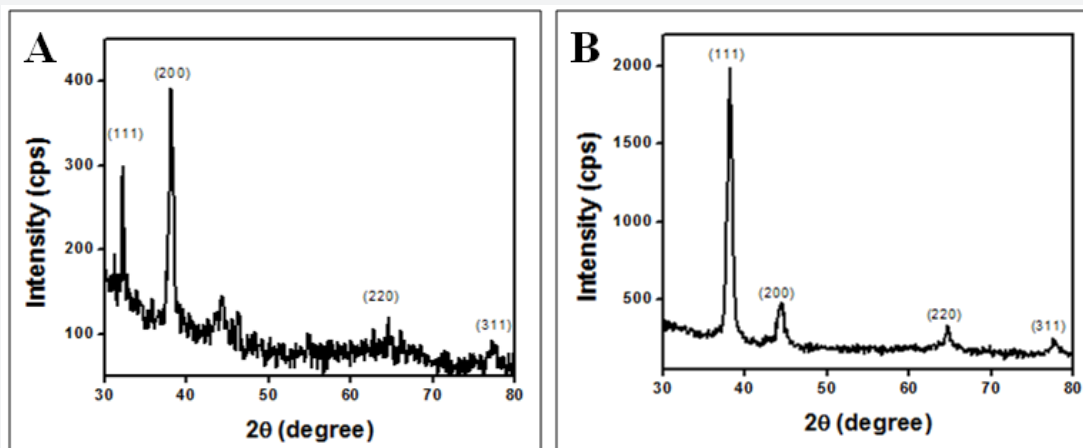


Figure 7: Representative X-ray diffraction profile of thin film AgNPs (A) and AuNPs (B) synthesized by LCPE.

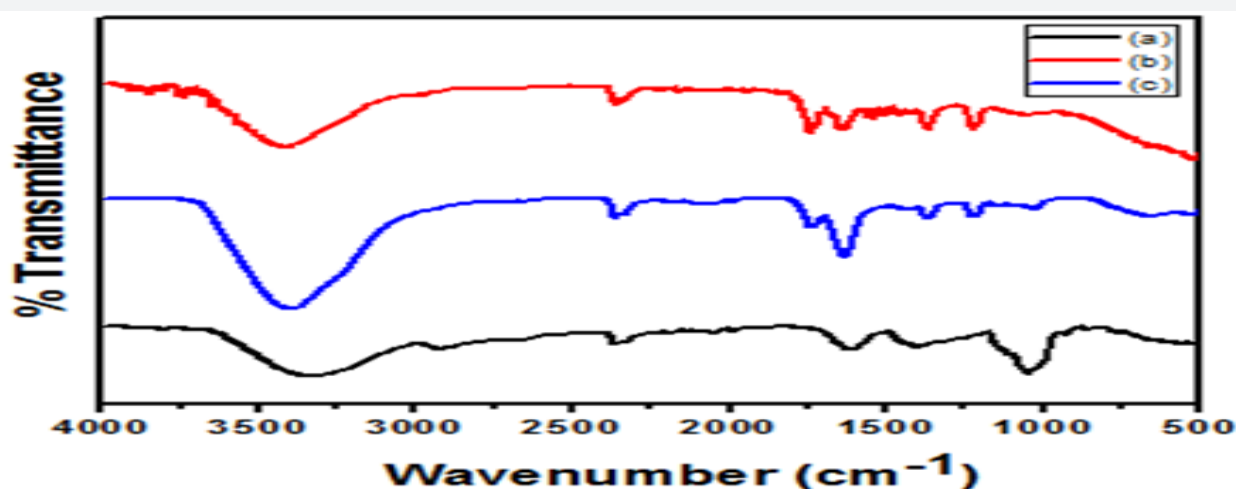


Figure 8: Fourier transform infrared absorption spectra of LCPE before bioreduction (a) and after complete bioreduction of AgNPs (b) and AuNPs (c).

Phytochemical analysis

Phytochemical estimation using various biochemical assays indicated the presence of diverse groups of phytoconstituents

like phenolics, starch, reducing sugars, ascorbic acid and citric acid (Table 1). Very high amount of reducing sugars and citric acid was observed in LCPE followed by starch, ascorbic acid and phenolics.

Table 1: Phytochemical composition of LCPE

Sample	Phytochemicals (µg/mL)				
	Phenolic content	Starch content	Reducing sugars	Ascorbic acid	Citric acid
LCPE	25.67	153.33	1250	94	1116.67

Table 2: Main compounds detected by GCMS/MS.

Sr. No.	Compound Name	Retention Time (sec)	Formula	Molecular Weight
1	Octadecane, 6-methyl-	9.62	C ₁₉ H ₄₀	268
2	Tertbutyloxyformamide, N-methyl-N-[4-(1-pyrrolidinyl)-2-butynyl]-	9.81	C ₁₄ H ₂₄ N ₂ O ₂	252
3	Decane, 4-methyl-	9.93	C ₁₁ H ₂₄	156
4	Undecane	11.03	C ₁₁ H ₂₄	156
5	Tetradecane, 2,6,10-trimethyl-	11.23	C ₁₇ H ₃₆	240
6	Erucic acid	11.79	C ₂₂ H ₄₂ O ₂	338
7	Octadecane, 3-ethyl-5-(2-ethylbutyl)-	12.81	C ₂₆ H ₅₄	366

8	Geranyl isovalerate	14.88	$C_{15}H_{26}O_2$	238
9	2-Myristynoyl pantetheine	15.11	$C_{25}H_{44}N_2O_5S$	484
10	2-Hexadecanol	15.88	$C_{16}H_{34}O$	242
11	Dodecane	16.18	$C_{12}H_{26}$	170
12	2-Myristynoyl pantetheine	16.61	$C_{25}H_{44}N_2O_5S$	484
13	Undecane, 2-methyl-	18.75	$C_{12}H_{26}$	170
14	Octadecane, 1-chloro-	19.64	$C_{18}H_{37}Cl$	288
15	α -acorenol	21.41	$C_{15}H_{26}O$	222
16	α -ylangene	21.99	$C_{15}H_{24}$	204
17	alfa.-Copaene	22.23	$C_{15}H_{24}$	204
18	Tetradecane	22.94	$C_{14}H_{30}$	198
19	Caryophyllene	23.64	$C_{15}H_{24}$	204
20	Formic acid, 3,7,11-trimethyl-1,6,10-dodecatrien-3-yl ester	24.81	$C_{16}H_{26}O_2$	250
21	1,2,4-Metheno-1H-indene, octahydro-1,7a-dimethyl-5-(1-methylethyl)-, [1S-(1 α ,2 α ,3 α ,4 α ,5 α ,7 α ,8S*)]-	25.41	$C_{15}H_{24}$	204
22	Isocaryophillene	25.65	$C_{15}H_{24}$	204
23	Pentadecane, 3-methyl-	28.16	$C_{16}H_{34}$	226
24	Isoaromadendrene epoxide	28.53	$C_{15}H_{24}O$	220
25	Hexadecane	29.02	$C_{16}H_{34}$	226
26	Octadecane	34.46	$C_{18}H_{38}$	254
27	n-Hexadecanoic acid	38.61	$C_{16}H_{32}O_2$	256
28	cis-Vaccenic acid	42.67	$C_{18}H_{34}O_2$	282
29	cis-10-Nonadecenoic acid	45.01	$C_{19}H_{36}O_2$	296
30	Spirost-8-en-11-one, 3-hydroxy-, (3 β ,5 α ,14 β ,20 β ,22 β ,25R)-	52.34	$C_{27}H_{40}O_4$	428
31	Phenol, 2,4-bis(1,1-dimethylethyl)-, phosphite (3:1)	55.06	$C_{42}H_{63}O_3P$	646
32	17.alfa.,21 β -28,30-Bisnorhopane	61.44	$C_{28}H_{48}$	384

GCMS/MS fingerprinting

Presence of diverse phytochemicals was detected in LCPE which actually might play a role in reduction and stabilization

of AgNPs and AuNPs. Thirty two different major compounds in LCPE included erucic acid, geranyl isovalerate, 2-hexadecanol, α -acorenol, tetradecane (Table 2).

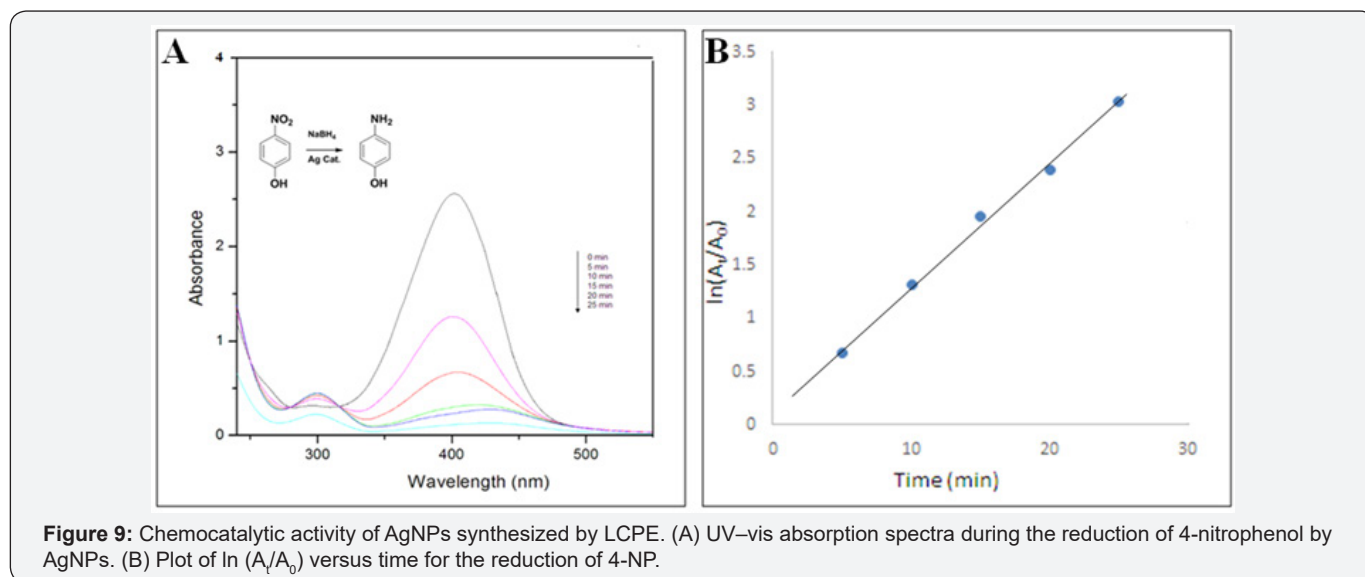


Figure 9: Chemocatalytic activity of AgNPs synthesized by LCPE. (A) UV-vis absorption spectra during the reduction of 4-nitrophenol by AgNPs. (B) Plot of $\ln(A_t/A_0)$ versus time for the reduction of 4-NP.

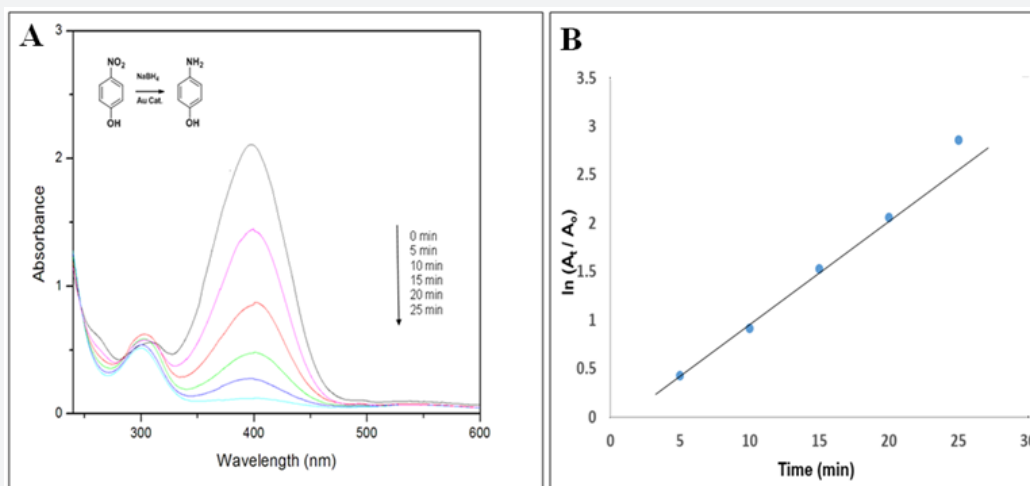


Figure 10: Chemocatalytic activity of AuNPs synthesized by LCPE. (A) UV-vis absorption spectra during the reduction of 4-nitrophenol by AuNPs. (B) Plot of $\ln(A_t/A_0)$ versus time for the reduction of 4-NP.

Catalytic activity

The catalytic performances of AgNPs and AuNPs nanoparticles were investigated by studying the reduction of 4-nitrophenol to 4-aminophenol by NaBH_4 . The reaction was found to be completed in 25min with $50\mu\text{L}$ of AgNPs. As seen from the Figure 9A, the absorption peak at 400nm gradually decreased in intensity as the reaction proceeded. At the same time, a new peak of 4-aminophenol at 295nm appeared with increasing intensity indicated the reduction of 4-NP. Thus, a linear relation between $\ln(A_t/A_0)$ versus time t has been obtained as shown in Figure 9B. The reactions followed pseudo-first order rate kinetics as the concentration of NaBH_4 used exceeded that of 4-NP and the AgNPs. This demonstrates a strong catalytic potential of AgNPs. The apparent rate constant (k) determined from this plot was $2.369 \times 10^{-4} \text{ min}^{-1}$, for AgNPs.

After addition of NaBH_4 , the absorption of 4-NP undergoes red shift from 317 to 400 nm due to formation of 4-nitrophenolate anion under alkaline condition that can be monitored spectrophotometrically. Reduction of $-\text{NO}_2$ group is possible only after the addition of catalytic amount of AuNPs. The addition of AuNPs to the solution causes a decrease in peak intensity at 400nm peak with appearance of a new peak at around 300nm which was attributed due to the synthesis of 4-AP as shown in Figure 10A. The reduction reaction was completed in 25min. The reactions followed pseudo-first order rate kinetics as the concentration of NaBH_4 was in excess. Thus, a good linear correlation was obtained between $\ln(A_t/A_0)$ vs time as seen in Figure 10B (A_t : absorbance at 400nm at time t , A_0 : absorbance at 400 nm at $t = 0$). The apparent rate constant (k) determined from this plot was $1.356 \times 10^{-4} \text{ min}^{-1}$, for AuNPs. Thus it was evident that the AuNPs possessed a strong catalytic potential.

Discussion

Among various active areas of material science, nanotechnology has received prime attention owing to the

newer applications of nanomaterials. Similarly, their self assembly and reaction parameters are monitored closely which reflects effectively. As a part of our constant efforts to study and develop environmentally benign processes, the present study demonstrated a rapid and efficient synthesis of AgNPs and AuNPs using LCPE. The synthesis was completed within 5h which was indicated by the visible colour change as well as the UV-visible spectra which was found to be faster as compared to *Cinnamomum camphora* leaf extract reported earlier [24]. Optimization studies indicated that salt concentration and reaction temperature has pronounce effects on the rate of synthesis of the nanoparticles. Our results are well in agreement with the report stating high temperature showed sharp increase in the synthesis of AgNPs and AuNPs using leaf extract of *Chenopodium album* [25]. Bioreduced AgNPs and AuNPs showed exotic shapes as revealed by HRTEM which were confirmed of their elemental composition using the EDS profile. Similar result were reported in case of synthesis of AuNPs and AgNPs using *Gnidia glauca*, *Plumbago zeylanica* and *Cinnamomum camphora* leaf extract [17,18,24] LCPE was found to contain polyphenols, reducing sugars, citric acid and ascorbic acid which may help in the bioreduction procedure while starch present in it might help in the stabilization. Our results are well supported by the earlier reports confirming the rich and diverse phytochemistry of *L. chinensis* [26] Unique phytochemistry of medicinal plants like *D. bulbifera*, *P. zeylanica*, *G. superba* and *B. prionitis* are reported to play a major role in the synthesis, stabilization and shape evolution of the nanoparticles. FTIR studies showed the existence of the peaks specific to various functional groups present in the diverse phytochemicals that may play a vital role in the bioreduction process. Appearance of the new peak indicates the O-H stretch [27-31]. This indirectly suggests the oxidation of the LCPE, reducing the metals salts into the respective metal nanoparticles. Further, GCMS studies have provided a strong rationale behind the synthesis of AgNPs and AuNPs by

identifying various compounds present in LCPE [12,17,19-21] Bio-reduced AgNPs and AuNPs exhibited superior chemocatalytic activity indicated by efficient reduction of 4-nitrophenol to 4-aminophenol. The reactions followed pseudo-first order rate kinetics as the concentration of NaBH_4 was in excess which was in agreement with previous reports on *Gnidia glauca* and *Breynia rhamnoides* [18,32] It is reported that such catalytic behaviour of nanomaterials are size and shape dependent [33-36]. Thus, it was observed that the AgNPs and AuNPs synthesized by LCPE can be of utmost industrial importance as well as can be used as novel nanobiotechnological model system to study various reaction parameters in order to achieve industrially significant metal nanoparticles using an eco-friendly rapid route.

Conclusion

In the present study, AgNPs and AuNPs were synthesized using *L. chinensis* peel extract which is a rapid, low cost and eco-friendly process. This single step procedure led to synthesis of stable and well dispersed nanoparticles which can further be used for large scale production owing to the optimization of reaction conditions like salt concentration and temperature. Interestingly, both AgNPs and AuNPs exhibited excellent chemocatalytic activity by reduction of 4-nitrophenol to 4-aminophenol at comparatively low concentration following a pseudo-first order rate kinetics. Based on the present findings, it can be concluded that AgNPs and AuNPs synthesized by LCPE are of immense industrial importance.

Acknowledgment

The authors acknowledge the help extended for the use of TEM and HRTEM facilities in Chemical Engineering and CRNTS funded by the DST through Nanomission and IRPHA schemes. Dr. Sougata Ghosh thanks STAR College Scheme, Department of Biotechnology, Government of India for support.

References

- Ghosh S, Nitnavare R, Dewle A, Tomar GB, Chippalkatti R, et al. (2015) Novel platinum-palladium bimetallic nanoparticles synthesized by *Dioscorea bulbifera*: Anticancer and antioxidant activities. *Int J Nanomedicine* 10: 7477-7490.
- Ghosh S, More P, Derle A, Kitture R, Kale T, et al. (2015) Diosgenin functionalized iron oxide nanoparticles as novel nanomaterials against breast cancer. *J Nanosci Nanotechnol* 15(12): 9464-9472.
- Mallick A, More P, Ghosh S, Chippalkatti R, Chopade BA, et al. (2015) Dual drug conjugated nanoparticle for simultaneous targeting of mitochondria and nucleus in cancer cells. *ACS Appl Mater Interfaces* 7(14): 7584-7598.
- Asok A, Ghosh S, More PA, Chopade B A, Gandhi M N, et al. (2015) Surface defect rich ZnO quantum dots as antioxidant inhibiting α -amylase and α -glucosidase: A potential anti-diabetic nanomedicine. *J Mater Chem B* 22(3): 4597-4606.
- Ghosh S, Parihar VS, More P, Dhavale DD, Chopade BA (2015) Phytochemistry and therapeutic potential of medicinal plant: *Dioscorea bulbifera*. *Med Che* 5(4): 154-159.
- Ghosh S, Parihar VS, Dhavale DD, Chopade BA (2015) Commentary on therapeutic potential of *Gnidia glauca*: A novel medicinal plant. *Med Chem* 5(8): 351-353.
- Ghosh S, Jagtap S, More P, Shete UJ, Maheshwari NO, et al. (2015) *Dioscorea bulbifera* mediated synthesis of novel $\text{Au}_{\text{core}}\text{Ag}_{\text{shell}}$ nanoparticles with potent antibiofilm and antileishmanial activity. *J Nanomater* 2015: 562938-5629410.
- Shalaka SR, Komal AJ, Ketakee M, Tomar G, Dubal DS, et al. (2017) Novel anticancer platinum and palladium nanoparticles from *Barleria prionitis*. *Glob J Nano* 2(5): 555600.
- Ghosh S, Patil S, Ahire M, Kitture R, Kale S, et al. (2012) Synthesis of silver nanoparticles using *Dioscorea bulbifera* tuber extract and evaluation of its synergistic potential in combination with antimicrobial agents. *Int J Nanomed* 7: 483-496.
- Ghosh S, Ahire M, Patil S, Jagunde A, Dusane MB, et al. (2012) Antidiabetic activity of *Gnidia glauca* and *Dioscorea bulbifera*: potent amylase and glucosidase inhibitors. *Evid Based Complement Alternat Med* 2012:929051.
- Ghosh S, More P, Derle A, Patil AB, Markad P, et al. (2014) Diosgenin from *Dioscorea bulbifera*: Novel Hit for treatment of Type II Diabetes Mellitus with inhibitory activity against α -Amylase and α -Glucosidase. *PLoS One* 9(9): e106039.
- Ghosh S, Derle A, Ahire M, More P, Jagtap S et al. (2013) Phytochemical analysis and free radical scavenging activity of medicinal plants *Gnidia glauca* and *Dioscorea bulbifera*. *PLoS One* 8(12): e82529.
- Kitture R, Ghosh S, More PA, Date K, Gaware S, et al. (2015) Curcumin-loaded, self-assembled *Aloe vera* template for superior antioxidant activity and trans-membrane drug release. *J Nanosci Nanotechnol* 15(6): 4039-4045.
- Kitture R, Chordiya K, Gaware S, Ghosh S, More PA, et al. (2015) ZnO nanoparticles-red sandalwood conjugate: A promising anti-diabetic agent. *J Nanosci Nanotechnol* 15(6): 4046-4051.
- Kitture R, Ghosh S, Kulkarni P, Liu XL, Dipaket, et al. (2012) Fe_3O_4 -citrate-curcumin: Promising conjugates for superoxide scavenging, tumor suppression and cancer hyperthermia. *J Appl Phys* 111: 064702-064707.
- Ghosh S, Patil S, Ahire M, Kitture R, Jagunde A, et al. (2012) Synthesis of gold nanoanisotrops using *Dioscorea bulbifera* tuber extract. *J Nanomater* 2011: 354793-354800.
- Salunke GR, Ghosh S, Santosh Kumar RJ, Khade S, Vashisth P, et al. (2014) Rapid efficient synthesis and characterization of silver, gold, and bimetallic nanoparticles from the medicinal plant *Plumbago zeylanica* and their application in biofilm control. *Int J Nanomedicine* 9: 2635-2653.
- Ghosh S, Patil S, Ahire M, Kitture R, Gurav DD, et al. (2012) *Gnidia glauca* flower extract mediated synthesis of gold nanoparticles and evaluation of its chemocatalytic potential. *J Nanobiotechnology* 10:17.
- Ghosh S, Gurav SP, Harke AN, Chacko MJ, Joshi KA, et al. (2016) *Dioscorea oppositifolia* mediated synthesis of gold and silver nanoparticles with catalytic activity. *J Nanomed Nanotechnol* 7: 398.
- Ghosh S, Chacko MJ, Harke AN, Gurav SP, Joshi KA, et al. (2016) *Barleria prionitis* leaf mediated synthesis of silver and gold nanocatalysts. *J Nanomed Nanotechnol* 7(4):1-7.
- Ghosh S, Harke AN, Chacko MJ, Gurav SP, Joshi KA, et al. (2016) *Gloriosa superba* mediated synthesis of silver and gold nanoparticles for anticancer applications. *J Nanomed Nanotechnol* 7:390.
- Sung Y, Yang WK, Kim HK (2012) Antiplatelet, anticoagulant and fibrinolytic effects of *Litchi chinensis* Sonn. extract. *Mol Med Rep* 5(3): 721-724.
- Wen L, You L, Yang X, Yang J, Chen F, et al. (2015) Identification of phenolics in litchi and evaluation of anticancer cell proliferation activity and intracellular antioxidant activity. *Free Radic Biol Med* 84: 171-184.

24. Huang J, Li Q, Sun D, Lu Y, Su Y, et al. (2007) Biosynthesis of silver and gold nanoparticles by novel sundried *Cinnanonum camphora* leaf. *Nanotechnology* 18: 105104-105114.
25. Dwivedi AD, Gopal K (2010) Biosynthesis of silver and gold nanoparticles using *Chenopodium album* leaf extract. *Colloids Surf A Physicochem chem Eng Asp* 369(1-3):27-33.
26. Zhao M, Yang B, Wang J, Li B (2006) Identification of the major flavonoids from pericarp tissues of lychee fruit in relation to their antioxidant activities. *Food Chem* 98(3): 539-544.
27. Pereira RMS, Andrades NED, Paulino N, Sawaya ACHF, Eberlin MN, et al. (2007) Synthesis and characterization of a metal complex containing naringin and Cu, and its antioxidant, antimicrobial, antiinflammatory and tumor cell cytotoxicity. *Molecules* 12(7): 1352-1366.
28. Madejova J, Bujdak J, Komadel P, Gates WP (1996) Preparation and infrared spectroscopic characterization of reduced-charge montmorillonite with various Li contents. *Clay Minerals* 31: 233-241.
29. Sahoo NG, Bao H, Pan Y, Pal M, Kakran M, et al. (2011) Functionalized carbon nanomaterials as nanocarriers for loading and delivery of a poorly water-soluble anticancer drug: a comparative study. *Chem Commun* 47(18): 5235-5237.
30. Coldea TE, Socaciu C, Fetea C, Ranga F, Pop RM, et al. (2013) Rapid quantitative analysis of ethanol and prediction of methanol content in traditional fruit brandies from romania, using FTIR spectroscopy and chemometrics. *Not Bot Horti Agrobio* 41(1): 143-149.
31. Ashokkumar R, Ramaswamy M. (2014) Phytochemical screening by FTIR spectroscopic analysis of leaf extracts of selected Indian Medicinal plants. *Int J Curr Microbiol App Sci* 3(1): 395-406.
32. Gangula A, Podila R, Ramakrishna M, Karnam L, Janardhana C, et al. (2011) Catalytic reduction of 4-nitrophenol using biogenic gold and silver nanoparticles derived from *Breynia rhamnoides*. *Langmuir* 27(24): 15268-15274.
33. Pradhan N, Pal A (2002) Pal A: Silver nanoparticle catalyzed reduction of aromatic nitro compounds. *Colloids Surf, A Physicochem Eng Asp* 196: 247-257.
34. Pfaff A, Shinde VS, Lu Y, Wittemann A, Ballauff M, et al. (2011) Mueller AHE: Glycopolymers-grafted polystyrene nanospheres. *Macromol Biosci* 11(2): 199-210.
35. Panigrahi S, Basu S, Praharaj S, Pande S, Jana S, et al. (2007) Synthesis and size-selective catalysis by supported gold nanoparticles: study on heterogeneous and homogeneous catalytic process. *J Phys Chem C* 111(12): 4596-4605.
36. Ghosh S, Patil S, Chopade NB, Luikham S, Kitture R, et al. *Gnidia glauca* leaf and stem extract mediated synthesis of gold nanocatalysts with free radical scavenging potential. *J Nanomed Nanotechnol* 7: 358.



This work is licensed under Creative Commons Attribution 4.0 License
DOI: [10.19080/GJN.2017.03.555603](https://doi.org/10.19080/GJN.2017.03.555603)

Your next submission with JuniperPublishers will reach you the below assets

- Quality Editorial service
- Swift Peer Review
- Reprints availability
- E-prints Service
- Manuscript Podcast for convenient understanding
- Global attainment for your research
- Manuscript accessibility in different formats
(Pdf, E-pub, Full Text, Audio)
- Unceasing customer service

Track the below URL for one-step submission

<https://juniperpublishers.com/submit-manuscript.php>